

CT analysis on mesoscopic structure of sandstone under acidic environment

RunKe Huo, Shuguang Li*, Fei Han & Guojie Wang

School of Civil Engineering, Xi'an University of Architecture and Technology, Xi'an710055, China

*[Email: lssgg2015@163.com]

Received 06 January 2017 ; revised 24 January 2017

Present study consists the mesoscopic structure of sandstone under acidic environment through CT analysis. Simulation of indoor accelerated corrosion test and CT nondestructive identification technology were applied to CT scanning test for the micro-structure of sandstone at different corrosion stages. It is found that as the extension of soak time, the CT number of wet sandstone samples in different stages trended to increase at first then decrease, the CT number of dry samples gradually decreased with extension of the soak time. The CT number variance of dry and wet samples were decreased first and then increased as soak time. CT images of the internal structure of wet and dry sandstone samples in the corrosion process were obtained and processed. Mass loss of sandstone in different corrosion stages was calculated. The variation of samples' quality and density, which were achieved from the experiment on the one hand and from the calculation of CT number on the other, were compared, and good agreement was achieved. Penetration depth of the sulfuric acid solution at different soak periods was deduced.

[Keywords: sandstone; acid corrosion; CT scan; corrosion mechanism; CT number; microscopic model]

Introduction

It is well established that the key point for meso-damage mechanics of rocks is the correct identification of meso-damage of rock materials, the discrepancy of mechanical properties of damaged rocks is the macroscopic manifestation of its characteristics, and this kind of macroscopic discrepancy is closely related to the change of its micro-structure. Environmental factors can cause internal damage to rocks, chemical reactions in the environment make the corrosion of rocks speed up, reduce rock strength, and ultimately lead to instability of rocks. CT, a kind of nondestructive test technology, can be used to the measurement of internal structure changes of rocks quantitatively, dynamically and non-destructively. X-ray computed tomography (CT scanner)^{1,2} has led to remarkable achievements in the field of medical science. In recent years, the development of industrial CT scanners has enabled observations to be made of the internal structure of rocks.

Raynaud et al.³ used an X-ray CT scanning system to image sample interiors without damaging the samples. Yang et al.^{4,5} introduced CT to the identification of rock damage for the first time, derived a formula to express the damage variable of rock with CT number, calculated and compared it

with Bellion's⁶ formula and Lemaitre's⁷ formula, for which the damage variable were expressed by material density, thereby verified the correctness of the formula of damage value of rock expressed by CT number, at the same time, they analyzed the law of damage propagation of rocks. Ding et al.⁸ divided damage evolution of rocks under uniaxial and triaxial compression, proposed the concept of density damage increment, analyzed the mechanical mechanism of the crack and monitored the width of the crack, established the relationship between the density damage increment and the volumetric strain. Yin et al.⁹ made the extraction of binary images of crack realized, and did fractal dimension, statistic and analysis of the evolution process images of the crack. Kawamura T.¹⁰ used X-ray computed tomography CT to observe non-destructively the internal structure of sea ice grown in the laboratory, compared the CT images with photographs taken by the conventional method and recognized both brine layers and brine drainage on the CT images. V. G. Ruiz de Argandoña et al.¹¹ used X-ray CT for imaging textural features and the internal pore structure of a dolomitic rock used as building material in Oviedo Cathedral, Spain. The reconstructed 3D image shows a non uniform distribution of porosity. They also studied the evolution of the void structure by X-ray CT. L. B.

Wang *et al.*¹² presented method of X-ray CT to quantify the specific damaged surface area, the specific damaged surface area tensor, the damage tensor, the mean solid path among the damaged surfaces and the mean solid path tensor, reconstructed three-dimensional structure from tomography images, obtained cross-sectional images with a virtual sectioning technique, and they also presented the relation between the quantified damage parameters and their applications in mechanical modeling. J. Geiger *et al.*¹³ made a analysis of small-scale heterogeneity in clastic rocks by using computerized X-ray tomography. Y. H. Han *et al.*¹⁴ established a numerical model of elastic properties for porous rocks based on CT-scanned images using direct mapping method, checked the numerical simulation results with laboratory experimental data.

In this paper, CT nondestructive technology was used to achieve the microstructure of the rocks at different corrosion stages, CT images of the internal structure of wet and dry sandstone samples in the process of corrosion were obtained, the distribution of three phase medium and the change of microstructure of rocks in different corrosion stages were monitored, which provide a basis for the accurate representation of the non-uniformity and the change of microstructure of the internal medium of corroded sandstone, and provide a new way to study the damage properties of sandstone that corroded by acid rain.

Materials and Methods

Test samples are dark gray particle containing calcium lithic feldspathic sandstone that taken from a hydraulic engineering in ShanXi province. These samples were removed from a large block of complete sandstone with the method of core sampling, then the samples were processed into standard cylindrical specimens with $h=100\text{mm}$, $\varphi=50\text{mm}$, in order to reduce the dispersion of the test results caused by individual differences in natural rock samples, wave velocity test was carried out, from which samples with larger or smaller wave velocity were excluded, thus specimens with the same physical and mechanical properties were obtained. Due to the number of samples is large, we choose the sample 1#, whose data is sufficient to explain the problem, as

example. The physical indexes of the specimen was tested, as shown in Table 1

Mineral compositions of sandstone samples were identified, mainly include quartz, feldspar, mica, chlorite, siliceous debris and limestone debris. Interstitial materials mainly include clay matrix and a small amount of calcite, silica, iron and chlorite cements, the particles are mainly supported by mutual support among themselves, which are in the forms of point contact and line contact, and the mainly form is porous cementation. The content of major mineral components is: quartz 58%, calcite 5%, feldspar 11%, mica 3%, detritus 8%, chlorite 1%, siliceous and ferruginous cements 7%, clayey 3%, however, heavy mineral epidote and apatite are rarely seen, samples are shown in Figure 1.

Test Equipment

The CT scan was tested on PHILIPS Brilliance 16-slice spiral CT machine in Key Laboratory of Frozen Soil Engineering, Cold and Arid Regions Environmental and Engineering Research Institute, Chinese Academy of Sciences. The main parameters were as follows: voltage 120kV, current 185mA, reconstruction matrix 1024×1024 , enlargement ratio 1, filter function EC, the thickness of scan layer is 3 mm. Scanning and positioning for samples are shown in Figure 2.

Sandstones for CT scan were dry and wet samples, which were soaked in sulphuric acid solution. The

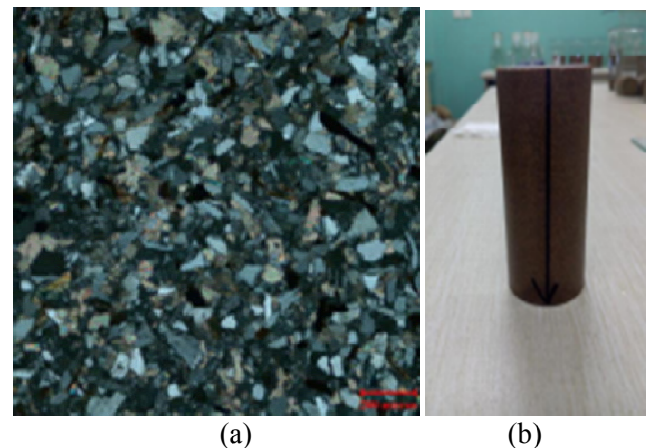


Fig. 1(a-b)—Image of meso-structure of sandstone sample and Image of sandstone sample (a) Image of meso-structure of sample and (b) Image of sandstone sample

Table 1—Basic physical parameter of the sandstone sample

NO.	Initial quality of sample (g)	Initial Porosity	Diameter (mm)	Height (mm)	Initial Dry Density of Samples(g/cm^3)	Volume(cm^3)
1#	515.74	2.03%	50	100	2.628	196.25

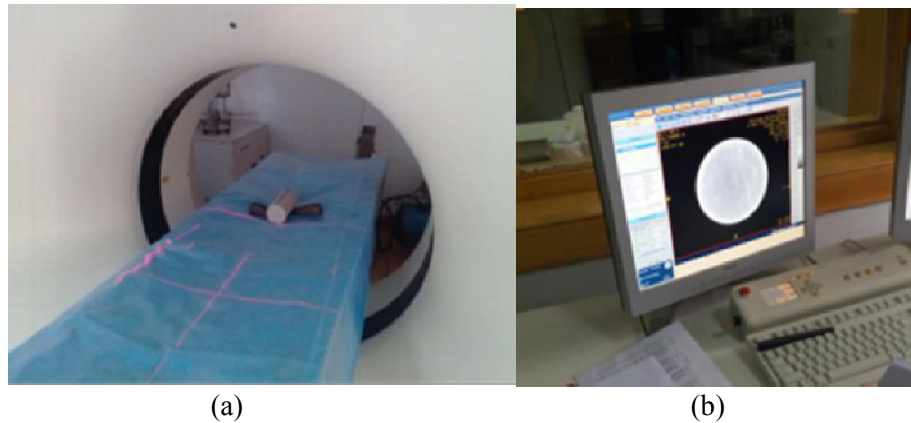


Fig. 2(a-b)— Spiral CT scanner and the scanning process (a) Scanning and Positioning for sample and (b) CT image

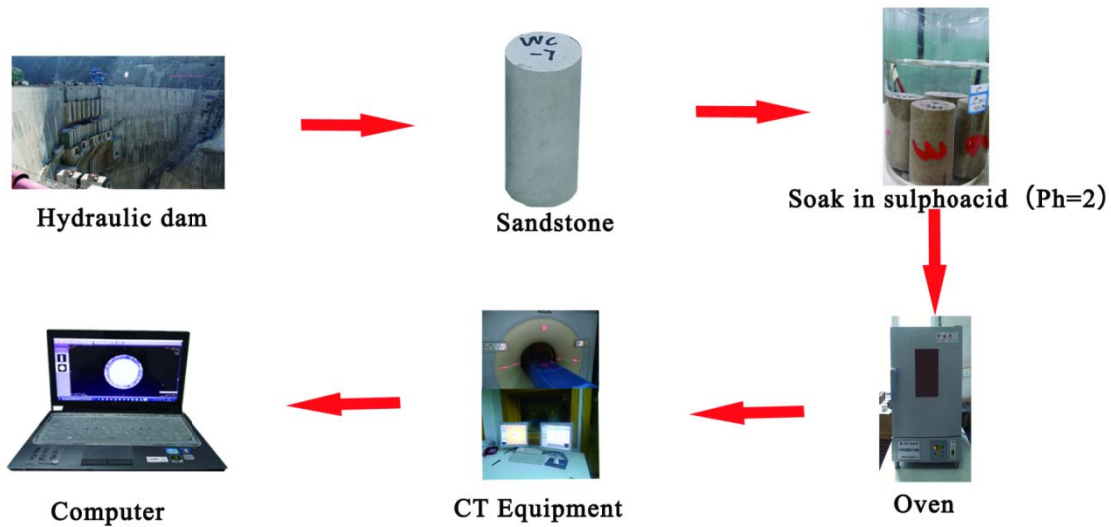


Fig. 3—The microstructure analysis system of sandstone

method of preparation for dry samples was that put the samples which were soaked in sulphuric acid solution for a certain period of time into the WGL-30B oven, baked them at 105°C for more than 24 hours to their constant weight, then weighed and recorded the quality of the wet and dry samples. the test system is shown in Figure 3.

Experimental procedure

CT scan test mainly applied to observe the internal micro-structure change of sandstone samples that were soaked in sulphuric acid solution (PH=2) in different period of time. The specific process of this experiment is as follows: ①Each of the scan layer of original sandstone samples was scanned continuously, then micro-structure of original sandstone and CT images were obtained. ②Sulphuric acid solution (PH=2) was

exchanged every 30d, when sandstone samples soaked in sulfuric acid solution in three phases (0~90d), took the wet samples out and did CT test for them, the CT images of internal micro-structure of corroded sandstone samples were observed, then put the wet sample into the oven for drying, put the dry samples on the scan bed and fixed it, did CT scan test for them as the way for wet samples, and CT images of different section of dry samples were obtained, then observed micro-structure change of sandstone after three stages of corrosion. ③Similarly, sandstone samples were soaked in sulfuric acid solution (PH=2), took them out after three stages (90~180d) and six stages (180~270d), made continuously CT scan test on wet and dry samples, then CT scan images and micro-structure of wet and dry samples corroded by sulfuric acid solution were obtained.

Results

In this test, CT scan images of sandstone samples in each corrosion stage were obtained, and then internal mesoscopic changes of sandstone samples were analyzed. In order to reduce the error caused by uneven infiltration at the top and bottom parts of specimens, the middle layer of sandstone samples was selected as the research object. Test results are listed in Table 2.

Discussion

CT images in the middle layer of sandstone samples soaked in sulphuric acid solution for different stages are shown in Figure 4.

The relationship between CT number and variance of sandstone and soak time

Test data of the middle layer of wet and dry samples soaked in sulfuric acid solution (PH=2) for different stages are shown in figure 5. It can be seen from figure 4 that as the extension of soak time, the CT number of wet sandstone samples in different stages trended to increase at first then decrease. After three stages (0~90d) of soaking, the CT number increased from 2150.02 to 2190.33, which is increased by 1.87%, and then decreased to 2155.68 after nine stages (0~270d) of soaking. In the process of soaking, voids of rock samples were filled with

Table 2—Test data in the middle layer of samples that soaked in sulfuric acid (PH=2) for different stages

S=19.6 (cm ²) ^a	Mean ^b	SD ^c	Max ^d	Min ^e	
Original sample	2150.02	270.09	2976	220	
After three stages of corrosion	Wet sample	2190.33	264.54	2976	187
	Dry sample	2128.57	262.6	2976	177
After six stages of corrosion	Wet sample	2175.18	274.31	2976	168
	Dry sample	2112.09	277.29	2976	142
After nine stages of corrosion	Wet sample	2155.68	280.35	2976	156
	Dry sample	2092.37	284.21	2976	114

S standard cross sectional area of scanning; Mean standard mean value of CT number, it would be represented by the CT number in the following description; SD standard variance of CT number; Max standard maximum value of CT number; Min standard minimum value of CT number

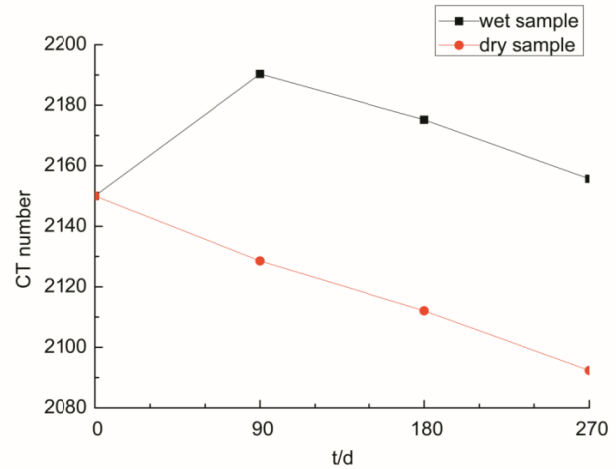


Fig. 5—CT number of wet and dry samples at different soak stages

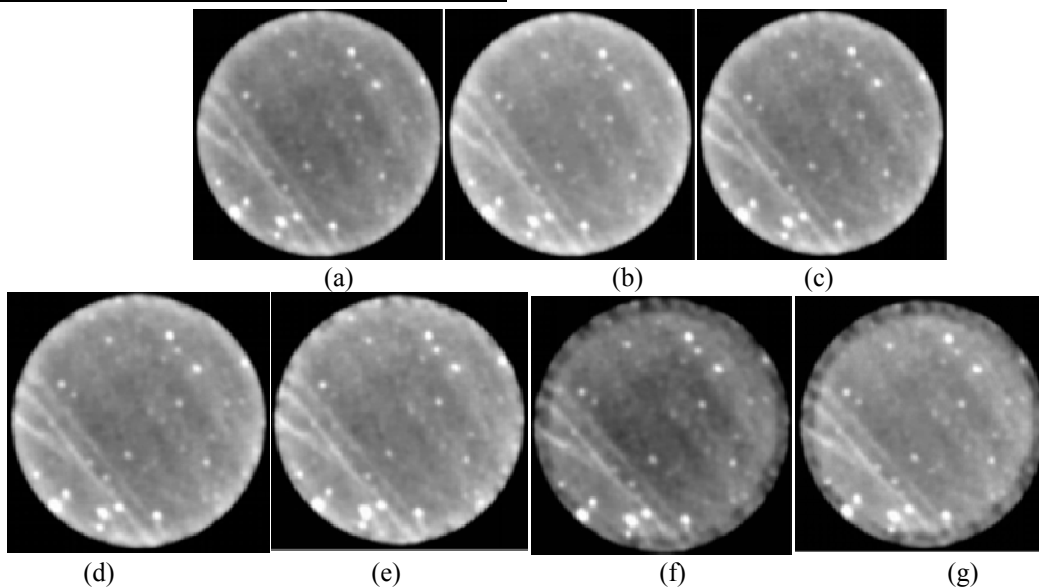


Fig. 4(a-g)—CT images of sandstone samples in different soak stages (a) Original sample; (b) Wet sample of soaking 90 days; (c) Dry sample of soaking 90 days; (d) Wet sample of soaking 180 days; (e) Dry sample of soaking 180 days; (f) Wet sample of soaking 270 days and (g) Dry sample of soaking 270 days

sulfuric acid solution, resulting in the increase of CT number of samples, at the same time, chemical effect can make the mineral composition react with sulfuric acid solution and dissolve the reactants into the solution, then reduce the density of the samples. When the diffusion effect was greater than the chemical reaction effect, CT number of the samples increase, but with the extension of soaking time, the strengthen of the chemical action played a leading role in the process, so the CT number fall down.

The CT number of dry samples gradually decreased with extension of the soak time. After the end of nine stages (0~270d) of soaking, the CT number was changed from the 2150.02 to 2092.37, reduced by 2.68%. This is because as the soak time went by, sulfuric acid solution continually react with the mineral composition of sandstone, a large number of pores and voids generated in the interior of the sandstone, which let to the decrease of sample density and CT number.

The main difference between the CT number of wet samples and dry samples, which were in the same soak stage, is wet sample pores were filled with solution while dry sample pores were filled with air. Figure.4 shows that once the nine stage of soaking was over, the difference of CT number for wet and dry samples have reached to the maximum of 76.23, the above shows that corrosion effect of the sulfuric acid solution made the mineral composition of rock samples dissolved gradually, then more and more voids were generated, and the difference value of CT number increase gradually.

CT number variance of middle layer of wet and dry samples that are soaked in different stages of sulfuric

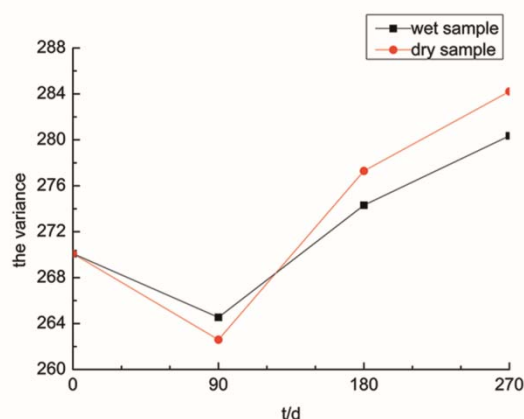


Fig. 6—CT number variance of wet and dry samples at different soak stages

acid solution (PH=2) are shown in figure 6. It can be seen that the the CT number variance of dry and wet samples were decreased first and then increased as soak time. After three stages (0~90d) of soaking, the CT number variance was reduced from 270.09 to the minimum values, which were 264.54 and 262.6 respectively. At the end of nine stages(0~270d), the CT number variance increased to the maximum value of 280.35 and 284.21 respectively, and the corresponding growth rates were 3.8% and 5.23% respectively, compared to the original samples. Chemical corrosive effect of the acid solution on sandstone samples dissolved part of the mineral components of rock samples, then internal mineral composition tend to homogenize, that is the reason why the variance of CT number decrease. However, the reason way CT number variance increase is the effect of the chemical corrosion of acid solution become violent, a large number of mineral in samples occurred chemical reaction and a lot of pores and voids generated in the interior of the sandstone, which increase the inhomogeneity of samples.

Mesomodel of sandstone that corroded by acid

Corrosion process of sandstone in acidic solution

In the corrosion process for sandstone in sulfuric acid solution, the interaction between the sandstone and the acid medium can be regarded as a multiphase process of physical and chemical, the corrosion process of sandstone from outside to inside can be divided into several stages: ①For sandstone soaked in sulfuric acid solution, when the acidic medium penetrate into its empty voids, the chemical reaction that carried out in the wet film on the surface of various defects of sandstone is faster, the corrosion mechanism of sandstone in sulfuric acid solution is mainly controlled by diffusion. ②When the speed of sandstone absorb acid medium is less than the penetration speed of medium, not all of the medium will be consumed in the corrosive area of sandstone, actually acidic medium controlled by chemical kinetics penetrate into the interior of the samples, then deeper reaction zones are formed.

Basic assumptions

In order to simplify the model, sandstone samples was considered to be isotropic homogeneous, effects of the two end faces of rock samples on diffusion were ignored, the spread of acid medium along the radial expansion, the scope of interaction between sandstone and acid solution was divided into three

zones: corroded area, reactive area and none corroded area, for convenient analyze, corroded area and reactive area were merged into a diffusion-affected area, as shown in Figure 7.

Calculation of filtering damage depth

Mineral composition of diffusion-affected area of sandstone sample soaked in sulfuric acid solution occurred chemical reaction with sulfuric acid and dissolved, then new holes and pores formed, which were completely filled by solution. Therefore the pore of diffusion-affected area in different soak stage is:

$$V_v = \frac{m}{\rho_0} \dots (1)$$

Where, standard pore of diffusion-affected area (cm³); standard the quality of damaged rock (g); standard initial density of sandstone sample.

After t hours of soaking in sulfuric acid solution, the ratio of pores in diffusion-affected area and pores in the whole sandstone sample is equal to the ratio of volume of diffusion-affected area and volume of the whole sandstone sample, that is:

$$\frac{V_v}{\alpha_0 V + V_v} = \frac{\frac{\pi}{4} h [d^2(0) - d^2(t)]}{\frac{\pi}{4} d^2(0) h} \dots (2)$$

Where, standard initial porosity of sandstone sample; standard diameter of the original sandstone sample (mm); standard diameter of corroded sandstone sample after t hours of soaking (mm); standard the height of sandstone sample (mm).

The following formula can be deduced from (1) and (2)

$$d(t) = \sqrt{1 - \frac{m_s}{\rho_0 \alpha_0 V + m_s}} d(0) \dots (3)$$

And then the depth of penetrative damage can be calculated as follows:

$$x(r, t) = \frac{1}{2} [d(0) - d(t)] = \frac{d(0)}{2} \left[1 - \sqrt{1 - \frac{m_s}{\rho_0 \alpha_0 V + m_s}} \right] \dots (4)$$

The relationship between CT number of wet and dry samples corroded by acid and density

Following assumptions were taken in deriving formulas: ①The dissolution of rock mineral caused empty pores become bigger, pores produced by chemical reaction in wet samples were all filled by solution, pores in dry samples were filled by air; ②Densities of solution and water were considered equal approximately; ③New empty pores produced by dissolving minerals were evenly distributed in diffusion-affected area of sandstone samples, effects of initial porosity of samples on diffusion-affected area were ignored.

First of all, volume influence coefficient, which is the ratio of sulfuric acid solution diffusion volume and the total sample volume, was defined as follows:

$$\beta = \frac{\frac{\pi}{4} h [d^2(0) - d^2(t)]}{\frac{\pi}{4} d^2(0) h} \dots (5)$$

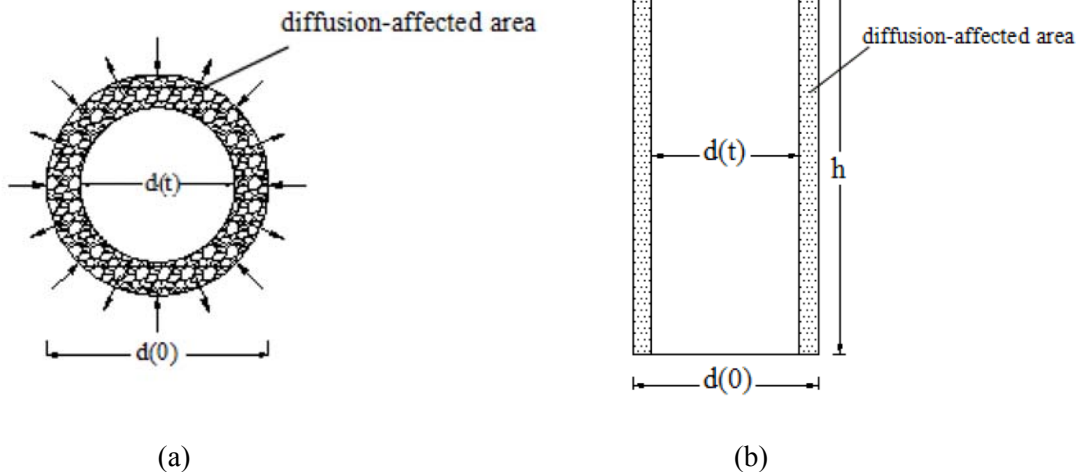


Fig. 7(a-b)—Penetrative and diffused model of sandstone samples (a) Cross section penetration of sample and (b) Longitudinal section penetration of sample

After a period time of soaking, empty pores were produced because of dissolving of the sample minerals, then new porosity, which is produced in diffusion-affected area of sample, can be expressed as follows:

$$\alpha_t = \frac{V_v}{\frac{\pi}{4}h[d^2(0)-d^2(t)]} = \frac{m_s}{\frac{\pi}{4}\rho_0h[d^2(0)-d^2(t)]} \dots (6)$$

By the CT machine principle, the size of the CT number of rock is directly proportional to the absorption of the X-ray by rock, the distribution law of H reflects the change of rock density essentially, that is:

$$H = a\mu + b \dots (7)$$

$$\mu = \mu^m \rho \dots (8)$$

Where, standard absorption coefficient of rock to X-ray and absorption coefficient of quality respectively; standard density of rock (g/cm³); are constants.

1. The pores of dry samples soaked in acid solution in different stage were filled up with air, then:

$$\mu = \rho\mu^m = \beta[(1-\alpha_t)\rho_r\mu_r^m + \alpha_t\rho_a\mu_a^m] + (1-\beta)[(1-\alpha_0)\rho_r\mu_r^m + \alpha_0\rho_a\mu_a^m] \dots (9)$$

Where, standard air in rocks and density of rock matrix material respectively; standard porosity of diffusion-affected area of rock samples after t hours of soaking; standard quality absorption coefficient of air in rock and quality absorption coefficient of matrix material respectively; standard initial porosity of rock. Simplified formula (9) as follows:

$$\mu = \alpha_t\beta(\rho_a\mu_a^m - \rho_r\mu_r^m) - (1-\beta)\alpha_0(\rho_r\mu_r^m - \rho_a\mu_a^m) + \rho_r\mu_r^m \dots (10)$$

Simultaneous equations (7), (8) and (10) as follows:

$$\alpha_0 = \frac{\alpha_t\beta(H_a - H_r) + H_r - H}{(1-\beta)(H_r - H_a)} \dots (11)$$

Where, standard density of rock (g/cm³); standard CT number of sample in different soaking stage; standard CT number of rock matrix; standard CT number of air, = -1000.

Density considered resolution cell can be written as follows:

$$\rho = \beta[(1-\alpha_t)\rho_r + \alpha_t\rho_a] + (1-\beta)[(1-\alpha_0)\rho_r + \alpha_0\rho_a] \dots (12)$$

Because of =0, formula (12) can be simplified as follows:

$$\alpha_0 = \frac{(1-\alpha_t\beta)\rho_r - \rho}{(1-\beta)\rho_r} \dots (13)$$

Simultaneous equations (11) and (13):

$$\rho = \frac{\alpha_t\beta H_r(\rho_r - 1) + \rho_r(H - H_a)}{H_r - H_a} \dots (14)$$

Assume that original sandstone samples are made up of matrix and pores, that is:

$$\rho_r = \frac{\rho_0}{1-\alpha_0} \dots (15)$$

$$H_r = \frac{H_0 - \alpha_0 H_a}{1-\alpha_0} \dots (16)$$

Where, standard CT number of initial sandstone samples. Then

$$\Delta\rho_i = \rho - \rho_0 = \frac{\alpha_t\beta H_r(\rho_r - 1) + \rho_r(H - H_a)}{H_r - H_a} - \rho_0 \dots (17)$$

Change of the quality of dry sandstone after different stages of soaking can be calculated from formula (17):

$$\Delta m_i = \Delta\rho_i V = \frac{\alpha_t\beta H_r(\rho_r - 1) + \rho_r(H - H_a)}{H_r - H_a} V - m_0 \dots (18)$$

Where, standard initial quality of sandstone sample (g); standard quantity of change of quality for dry sandstone sample (g); standard quantity of change of density for dry sandstone sample (g/cm³); standard volume of sandstone sample (cm³).

The calculated results are shown in Table 3, in which minus sign indicates the decrease of the density and quality.

The pores of wet samples soaked in different stages in diffusion-affected area of rock are filled up with solution, pores that were not corroded were filled up with air, then:

Table 3—Change of physical quantity of dry samples that soaked in different stages of PH = 2 sulfuric acid solution

Soaking time	Volume influence coefficient	Density/ (g/cm ³)	Quantity of change of density/ (g/cm ³)	Quality/ (g)	Quantity of change of quality/(g)
Three stages (0~90d)	0.182	2.615	-0.013	513.19	-2.55
Six stages (0~180d)	0.289	2.605	-0.023	511.23	-4.51
Nine stages (0~270d)	0.381	2.594	-0.034	509.07	-6.67

$$\mu = \rho\mu^m = \beta[(1 - \alpha_t)\rho_r\mu_r^m + \alpha_t\rho_w\mu_w^m] + (1 - \beta)[(1 - \alpha_0)\rho_r\mu_r^m + \alpha_0\rho_a\mu_a^m] \dots (19)$$

Where, standard density of water (g/cm³) ; standard density of air (g/cm³) ; standard quality absorption coefficient of water inside of the rock.

Simplified formula (19) as follows:

$$\mu = \alpha_t\beta(\rho_w\mu_w^m - \rho_r\mu_r^m) - (1 - \beta)\alpha_0(\rho_r\mu_r^m - \rho_a\mu_a^m) + \rho_r\mu_r^m \dots (20)$$

Similarly, the change of density of wet sandstone can be obtained as follows:

$$\Delta\rho_j = \rho - \rho_0 = \frac{H_a - H - \alpha_t\beta H_a}{H_a - H_r} \rho_r - \rho_0 \dots (21)$$

Changes of quality of wet sample that soaked in different stages can be calculated from formula (21) as follows:

$$\Delta m_j = \Delta\rho_j V = \frac{H_a - H - \alpha_t\beta H_a}{H_a - H_r} \rho_r V - m_0 \dots (22)$$

Where, standard quantity of change of quality for wet sample(g); standard quantity of change of density for wet sample (g/cm³).

The calculated results are shown in Table 4, in which minus sign indicates the decrease of the density and quality.

Verification of CT number of sandstone corroded by acid solution and density equation

Verification of CT number of dry sandstone corroded by acid and density relation

After different stages of soaking in sulfuric acid solution, the sandstone samples were taken out and dried in baking box for at least 24 hours until its quality were not change, then weighed them with electronic balance (whose scale value is 0.01g). The density and quality changes in different stages of dry samples were obtained respectively according to calculate of the CT number and weigh of electronic balance, which are shown in Table 5.

The following conclusions can be drawn through comparison: ① The qualities of samples soaked in different stages obtained from CT number are bigger

than that of weighing from electronic balance, because there are more minerals in both sides of rock sample react with sulfuric acid solution, yet CT number of relatively stable intermediate layer are selected to scan, whose value is bigger than average CT number of the whole sandstone samples. When such values are used to calculate quality of rock samples, the calculated quality will be bigger. Moreover, in addition to the mass consumption of feldspar, black mica and calcium carbonate, other mineral components have also been measured to participate in the reaction, which to some extent will also affect the accuracy of the calculation. ② The following conclusions can be obtained from the comparison of ρ_a and ρ_b , the difference of ρ_a and ρ_b are 0.1%, 0.3% and 0.4% respectively after three stages (0~90d), six stages (0~180d) and nine stages (0~270d), which proved that density changes of sandstone sample obtained from calculating of CT number have good consistency with the density changes obtained from weighing.

Verification of CT number of wet sandstone corroded by acid solution and density relation

The densities and qualities in different stages of dry samples were obtained respectively according to

Table 5—Physical quantities of dry sandstone in different stages were obtained from CT number and electronic balance

Soak time	ρ_a / (g/cm ³) ^a	ρ_b / (g/cm ³) ^b	m_a / (g) ^c	m_b / (g) ^d
Three stages (0~90d)	2.615	2.614	513.19	512.95
Six stages (0~180d)	2.605	2.602	511.23	510.66
Nine stages (0~270d)	2.594	2.590	509.07	508.19

ρ_a standard density of dry sandstone soaked in different stages, which were obtained from the calculation of CT number

m_a standard quality of dry sandstone soaked in different stages, which were obtained from the calculation of CT number

ρ_b standard density of sandstone soaked in different stages, which were obtained from weighing of electronic balance

m_b standard quality of sandstone soaked in different stages, which were obtained from weighing of electronic balance

Table 4—Change of physical quantity of wet samples that soaked in different stages of PH = 2 sulfuric acid solution

Soaking time	Volume influence coefficient	Density / (g/cm ³)	Quantity of change of density / (g/cm ³)	Quality / (g)	Quantity of change of quality / (g)
Three stages (0~90d)	0.182	2.657	0.029	521.44	5.69
Six stages (0~180d)	0.289	2.642	0.014	518.49	2.75
Nine stages (0~270d)	0.381	2.622	-0.006	514.57	-1.18

Table 6—Physical quantities of wet sandstone in different stages were obtained from CT number and electronic balance

Soak time	ρ_c / (g/cm ³) ^a	ρ_d / (g/cm ³) ^b	m_c / (g) ^c	m_d / (g) ^d
Three stages (0~90d)	2.657	2.663	521.44	522.1
Six stages (0~180d)	2.642	2.656	518.49	520.64
Nine stages (0~270d)	2.622	2.647	514.57	518.15

ρ_c standard density of wet sandstone soaked in different stages, which were obtained from the calculation of CT number

m_c standard quality of wet sandstone soaked in different stages, which were obtained from the calculation of CT number

ρ_d standard density of sandstone soaked in different stages, which were obtained from weighing of electronic balance

m_d standard quality of sandstone soaked in different stages, which were obtained from weighing of electronic balance

calculate of the CT number and weigh of electronic balance, which are shown in Table 6.

The following conclusions can be drawn through comparison: ① m_c is little than m_d after different stages of soaking, that's because, in addition to Na^+ , K^+ , Mg^{2+} , Ca^{2+} , there exists other minerals participate in chemical reactions to produce ions dissolved into the solution in the process of soaking, which make the measured loss of consumed samples down, and then affect the accuracy of the calculation to some extent; ② The following conclusions can be obtained from the comparison of ρ_c and ρ_d , the difference of ρ_c and ρ_d are 0.23%, 0.53% and 0.95% respectively after three stages (0~90d), six stages (0~180d) and nine stages (0~270d), which proved that density changes of sandstone sample obtained from calculating of CT number have good consistency, but the error increase obviously.

Conclusions

In this paper, Brilliance 16 spiral CT scanner was introduced with the goal of doing CT scanning test for the micro-structure of sandstone at different corrosion stages, the relationship between CT number and variance of sandstone in different soak periods and time was analyzed, the following conclusions were driven:

The CT number of wet sandstone samples in different stages trended to increase at first then decrease. After three stages (0~90d) of soaking, the CT number increased from 2150.02 to 2190.33, which is increased by 1.87%, and then decreased to 2155.68 after nine stages (0~270d) of soaking. The CT number of dry samples gradually decreased with extension of

the soak time. After the end of nine stages (0~270d) of soaking, the CT number was changed from the 2150.02 to 2092.37, reduced by 2.68%.

The CT number variance of dry and wet samples were decreased first and then increased as soak time. After three stages (0~90d) of soaking, the CT number variance was reduced from 270.09 to the minimum values, which were 264.54 and 262.6 respectively. At the end of nine stages(0~270d), the CT number variance increased to the maximum value of 280.35 and 284.21 respectively, and the corresponding growth rates were 3.8% and 5.23% respectively compared to the original samples.

With the aid of the non-disturbed CT scanning technique and the use of chemical kinetic analysis. The micro-damage of sandstone corroded by acid solution was analyzed and quantified. The mass loss of sandstone sample in different corrosion stages was obtained. The penetration depth of the sulfuric acid solution at different soak periods was deduced. The functional relationship with the depth of corrosion, CT numbers and density of rock specimens was established.

Through preliminary verification of the variation of the mass and the density of dry and wet sandstone samples in different stages, following conclusions were given: density changes of sandstone sample obtained from calculating of CT number have good consistency with that obtained from weighing; Density changes of sandstone sample obtained from calculating of CT number have good consistency, but the error increase obviously.

Acknowledgment

This work was Supported by National Natural Science Foundation of China (NO.41172337).

References

- Hounsfield, G.N., Computerized transverse axial scanning (tomography), 1, Description of system. *Br. J. Radiol.*, 46 (1973) 1016-1022.
- Ledley, R.S., Di,C.G., Luessenhop, A.J., and Twigg, H.L., Computerized transaxial X-ray tomography of the human body. *Science*, 186 (1974) 207-212.
- Raynaud, S., Fabre, D., Mazerolle, F., Geraud, Y., and Latière, H.J., Analysis of the internal structure of rocks and characterization of mechanical deformation by a non-destructive method: X-ray tomodensitometry. *Tectonophysics*, 159(1989) 149-159.
- Yang, G.S., Xie, D.Y., and Zhang, C.Q., Rock damage characteristics of CT recognition. *Chinese Journal of Rock Mechanics and Engineering*, 15(1996)48-54.
- Yang, G.S., Xie, D.Y., and Zhang, C.Q., A quantitative analysis of rock damage CT number distribution. *Chinese*

- Journal of Rock Mechanics and Engineering*, 17 (1998) 279-285.
- 6 Bellion, G., and Bernaseoin, G., In creep of engineering. *Material & Structure*, 8 (1978) 54-65.
 - 7 Lemattre, J., Damage measurements. *Engineering Fracture Mechanics*, 28 (1987) 643-660.
 - 8 Ding, W.H., Wu, Y.Q., Pu, Y.B., and Liao, Q.R., The Density Damage Increment and Its Digital Image of Rock in Compression. *Journal of Xi'an University of Technology*, 16 (2000) 45-48.
 - 9 Yin, X.T., *Based on image quantitative analysis of sandstone damage mesoscopic mechanism research*, Master thesis, Xi'an University of Science, Xi'an, 2005.
 - 10 Kawamura, T., Observations of internal structure of sea ice by X-ray computed tomography. *Journal of Geophysical Research*, 93 (1998) 2343-2350.
 - 11 de Argandoña, V.G.R., Rey, A.R., Celorio, C., Río, L.M.S., Calleja, L., and Llavona, J., Characterization by computed X-ray tomography of the evolution of the pore structure of a dolomite rock during freeze-thaw cyclic tests. *Physics and Chemistry of the Earth, Part A : Solid Earth and Geodesy*, 24(1999)633-637.
 - 12 Wang, L.B., Frost, J.D., Voyiadjis, G.Z., and Harman, T.P., Quantification of damage parameters using X-ray tomography images. *Mechanics of Materials*, 35 (2003) 777-790.
 - 13 Geiger, J., Hunyadfalvi, Z., Bogner, P., Analysis of small-scale heterogeneity in clastic rocks by using computerized X-ray tomography(CT). *Engineering Geology*, 103 (2009) 112-118.
 - 14 Han, Y.H., Hu, D.D., and Matzar, L., Numerical computation of elastic properties for porous rocks based on CT-scanned images using direct mapping method. *Journal of Petroleum Science and Engineering*, 122 (2014) 346-353.